**PAPER**

# Superposition of low-pressure DBD and RF induction discharge for spectroscopic study of dissociative recombination in decaying plasma

View the article online for updates and enhancements.

# Superposition of low-pressure DBD and RF induction discharge for spectroscopic study of dissociative recombination in decaying plasma

**V A Ivanov**

St. Petersburg State University, St. Petersburg, 198504 Russia

E-mail: v.a.ivanov@spbu.ru

## Abstract

The aim of the work was to find the optimal way to set up an experiment for spectroscopic study of the dissociative recombination of molecular ions with electrons in low electron density plasma at low gas pressure. In such an experiment, the influence of inelastic atom–atom collisions on the distribution of the DR flux over the excited atomic levels can be excluded. The first results of an experiment on combining a low-frequency barrier discharge (DBD) in neon at a pressure of less than 1 Torr with a pulsed radio-frequency (RF) induction discharge are presented. To create the plasma, we used DBD in a cylindrical glass tube with an inner diameter of 3.9 cm, which forms the spatial distribution of electron density with a minimum on the axis of the tube. The evolution of such a spatial distribution due to ambipolar diffusion in the initial stage of plasma decay provides an influx of charged particles to the center of the discharge tube, which increases the afterglow duration and helps to overcome the difficulties of detecting weak plasma radiation. The specific features of the DBD also appeared in the ionic composition of the plasma, which contained, in addition to $Ne^+$ and $Ne_2^+$, the $Ne^{++}$ ions, whose recombination with electrons significantly enriched the afterglow spectrum in the short-wavelength region. An RF discharge was used for pulsed heating of electrons in the afterglow. It is shown that, in accordance with the ionic composition, the radiation of a decaying plasma is presented by three groups of spectral lines with characteristic time behavior and the electron temperature dependence. The advantages of the proposed approach for studying the mechanism of dissociative recombination are discussed.

Keywords: dielectric-barrier discharge, low-pressure plasma, optical emission spectroscopy, dissociative recombination, molecular ions, radio-frequency discharge, collisional-radiative recombination

## 1. Introduction

Dissociative recombination (DR) of molecular ions with electrons is one of the most important processes in low-temperature plasma. The study of this process, begun in [1], is actively ongoing at the present time [2, 3]. DR forms plasma parameters, on the one hand, as the fastest deionization mechanism (the DR cross section for many ions exceeds $10^{-13}$ cm$^2$ for thermal particles), and on the other hand, as an intense source of population of excited atomic states

$$R_2^+ + e \rightarrow \left(R_2^*\right)_{\text{unstable}} \xrightarrow{\alpha_j} R^*(j) + R + E_j^{\text{kin}}. \quad (1)$$
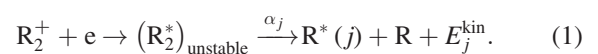
A molecular ion in a particular vibrational state captures an electron to form an unstable excited molecule which dissociates, producing two atoms, one in an excited state $R^*(j)$,

moving apart with kinetic energy depending on the states of particles in input and output channels of the reaction. For many applications, including the construction of recombination lasers [4], the data on the partial recombination coefficients $\alpha_j$ are of primary importance. They characterize the distribution of the total recombination flux

$$F_{\sum} = R_2^+[e] \sum a_j \qquad (2)$$

over the excited states of the atom. The recombination rate constants (coefficients) $\alpha = \sum \alpha_j$ at room electron temperature change from $1.7 \times 10^{-7}$ for $Ne_2^+$ to $2 \times 10^{-6}$ cm$^3$ s$^{-1}$ in the case of $Xe_2^+$ [5–8] and are characterized by a temperature dependence close to $T_e^{-0.5}$. Molecular ions in the plasma of noble gases are formed in three processes, two of which occur with the participation of a neutral atom

$$R^+ + R + R \xrightarrow{\beta} R_2^+ + R \qquad (3)$$

$$R^* + R \rightarrow R_2^+ + e. \qquad (4)$$
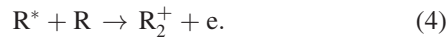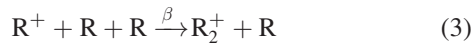
The characteristic values of the conversion coefficient in three-particle collisions are $\beta \approx 10^{-31}$ cm$^6$ s$^{-1}$ [9–12]. As for the associative ionization process (4), which was first studied in mass spectrometric experiments [13], its role in the balance of the number of charged particles is significant only at fairly high pressures, when the probability of collisions (4) (cross section $\sigma \approx 10^{-15}$ cm$^2$ [9, 14]) is comparable with the probability $1/\tau_{rad}$ of radiative decay of $R^*$ atoms.

Taking for estimation $\tau_{rad} \approx 10^{-7}$ s, we find that these probabilities are of the same order of magnitude at an atomic density $[R] \approx 10^{18}$ cm$^{-3}$. Thus, at pressures of tens of Torr, due to processes ((3) and (4)), the ionic composition of the plasma is such that $[R_2^+] \gg [R^+]$. A different situation occurs at low pressures, which are of interest in terms of the objectives of this work, when processes ((3) and (4)) are replaced by ionizing collisions between metastables $R^*_M$ [15]

$$R_M^* + R_M^* \xrightarrow{\delta} \begin{matrix} \xrightarrow{\delta_1} R^+ + R + e \\ \xrightarrow{\delta_2} R_2^+ + e \end{matrix}. \qquad (5)$$
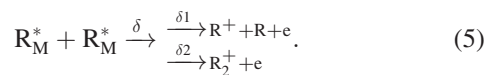
As an estimate of the rate constant $\delta$, a value of $10^{-9}$ cm$^3$ s$^{-1}$ can be taken [16], and the ratio $\delta_2/\delta_1 \approx 0.1$ [17]. A rough estimate of the relative density of molecular ions in the afterglow plasma under these conditions can be obtained by considering the quasistationary balance of their densities

$$[R_M]^2 * \delta * 0.1 \approx [R_2^+] * \alpha[e] \qquad (6)$$

([e] is the electron density).

Considering that in a plasma of noble gases created by pulsed DC or microwave discharges, the densities of metastable atoms and electrons are of the same order of magnitude ($[R_M] \approx [e]$[1]), from (6) we obtain

$$[R_2^+]/[e] \approx \delta * 0.1/\alpha \approx 10^{-3}. \qquad (7)$$

From this estimate, it is clear that the solution of the problem of studying the DR in a spectroscopic experiment is significantly complicated with a decrease of gas pressure.

Literature data on excited atoms appearing due to DR were obtained by several groups of researchers in three types of experiments:

(a) Interferometric study of the spectral lines profiles in the afterglow plasma [19–21]. In experiments [19, 20], a distinct Doppler broadening of a number of Ne and Ar lines was detected. The effect is due to the 'fast' atoms with $E_j^{kin}/2$ energies appearing in the afterglow as a result of DR. The authors of [21] succeeded in detecting the Doppler line broadening in a stationary discharge against the background of stepwise population of excited levels of Ne atom by electrons.

(b) Optical emission spectroscopy (OES) of the afterglow of DC or microwave discharges [9–12, 22–25].

(c) Time-of-flight spectroscopy of final product states of dissociative recombination based on determination of the kinetic energies of atoms released in the process [26, 27].

In these studies, as well as in similar studies of the decaying plasma of heavy noble gases (we refer the reader to the review [28] for details), it was found that DR populates excited levels of $np^5 (n + 1)p$, $np^5 (n + 1)d$ and $np^5(n + 2)p$ configurations ($n$ is the principal quantum number of an unexcited electron). According to [26, 27], $np^5 (n + 1)s$ and the ground state should be added to this set, however, we will not discuss these states in this paper, since their analysis is beyond the scope of the spectroscopic experiment.

A common drawback of most of the works cited above is the lack of analysis of the following two factors. First, the determination of the partial recombination coefficients $\alpha_j$ from spectroscopic observations should be based on the results of an experiment performed at a low gas pressure to excludes the 'mixing' of excited states in atomic collisions

$$R_k^* + R \rightarrow R_j^* + R. \qquad (8)$$

According to [25], in the case of neon, the gas pressure should not exceed several tenths of a Torr, while experiments [19–24] were performed at much higher pressures. For heavy noble gases, this estimate will be even more critical due to the more compact arrangement of the excited levels. In this regard, works using time-of-flight spectroscopy compares favorably with others: the gas pressure in the experiments [26, 27] did not exceed 20 mTorr, which excluded the influence of processes (8). It is interesting that in [27] the authors did not find neon atoms in three excited states of the Ne $2p^53p$ configuration, although all spectral lines belonging to the allowed $3p \rightarrow 3s$ transitions are registered in sited above spectroscopic experiments. This once again indicates the need for revision of the available data. Note that there is still no information on the role of DR in population of the $np^5 (n + 2)s$ levels. Second, in determining $\alpha_j$, cascade transitions should be taken into account

$$R_k^* \rightarrow R_j^* + h\nu_{kj}.$$

---

[1] An exception is helium plasma, in which the density of metastable He($2^3S_1$) atoms can be an order of magnitude higher than [e] [18].
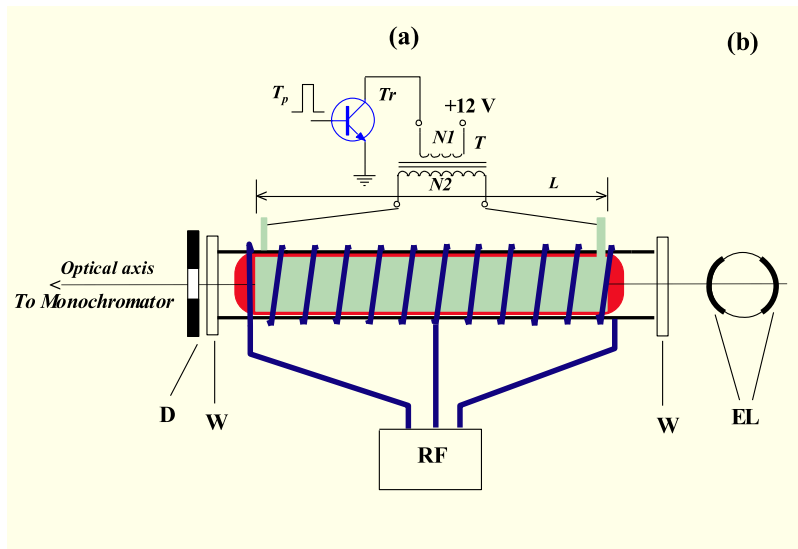
**Figure 1.** (a) Schematic of the set-up used in the experiments. W—quartz windows, D—diaphragm 5 mm in diameter. (b) The location of the DBD electrodes on the external side surface of the tube.

As far as we know, the only attempt to take into account cascade transitions in solving the problem under consideration was undertaken in [24]. The authors took concidered the 3d → 3p transitions in calculating the $\alpha_{3p}$ values for the Ne$_2^+$ ion. However, the role of transitions from 4p levels remains unclear, the lower of which are also populated by DR of Ne$_2^+$ ions [25]. In addition, the experiment [24] was performed at a pressure of 10 Torr, but the effect of the pressure on populations has not been studied. It follows from the foregoing that, despite more than a seventy-year history of the study of DR and the availability of a huge amount of data on the recombination of 2, 3, 4, …, 12-atomic molecular ions [29], important spectroscopic information about the simplest 2-atomic molecular ions of noble gases is so incomplete that it does not allow to predict with certainty the optical properties of the recombining plasma.

The main difficulty in determining the values of $\alpha_j$ is the necessity of setting up an experiment both at low pressure and at low electron density. At pressures less than 1 Torr, the main mechanisms of molecular ion formation ((3) and (4)) are so inhibited that atomic ions turn out to be the main ions in the plasma. Their recombination with electrons

$$R^+ + e + e \xrightarrow{\alpha_{cr}} R* + e \tag{9}$$
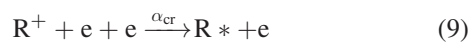
($\alpha_{cr}$—coefficient of collisional-radiative recombination). creates a flux of formation of excited atoms competing with DR (1). Under these conditions, plasma decay is mainly associated with the ambipolar diffusion of charged particles [19, 24].

The practice of the experiment shows [19] that, with a decrease in pressure to values less than 1 Torr, the detection of radiation caused by DR is associated with solving the problem of measuring extremely weak light fluxes with a time resolution. For example, obtaining data on the population of neon

4p levels [25] at a neon pressure of 0.6 Torr required measurements of the emissions of the 4p → 3s transition in the afterglow using the multichannel photon counting technique during $10^5$ to $10^6$ periods of a pulsed discharge at a frequency of less than 100 Hz. In this paper, we propose an experimental set-up that allows one to significantly advance into the low-pressure region when studying electron-ion recombination processes and, thus, to approach the solution of the problem of partial DR coefficients.

## 2. Experiment

To solve this problem, we turned to the barrier discharge in a cylindrical glass tube [30] as a way to create a low-pressure plasma. The geometry of the discharge is shown in figure 1. In this discharge, the amplitude of the current density corresponded to typical values of the glow DBD discharge [31, 32] with the average value equal to zero. The discharge current consists of two half-waves of positive and negative polarity with a duration of 2–3 $\mu$s. Each of them creates a plasma mainly near the cathode, so that as a result the plasma turned out to be diffuse, completely covering inner surfaces of the discharge tube adjacent to both electrodes. As electrodes (EL, figure 1(b)), we used strips of aluminum foil with a length of $L = 20$ and a width of 5 cm placed on the side surfaces of the tube with an inner diameter of 3.9 cm and a wall thickness of 2 mm. The gaps between the electrodes about 1 cm wide prevented electrical breakdown on the glass surface. The primary winding of the flyback transformer ($T$ in figure 1) is driven by a transistor IRG4PC50UD from a 12 V DC supply. With the ratio of the number of turns in the transformer $N_2/N_1 = 20$, this circuit could generate a voltage at the electrodes of up to 12 kV, which was enough to form a DBD at a neon pressure up to several hundred Torr in a tube of the used size. At gas pressures less than 1 Torr, plasma decay, as
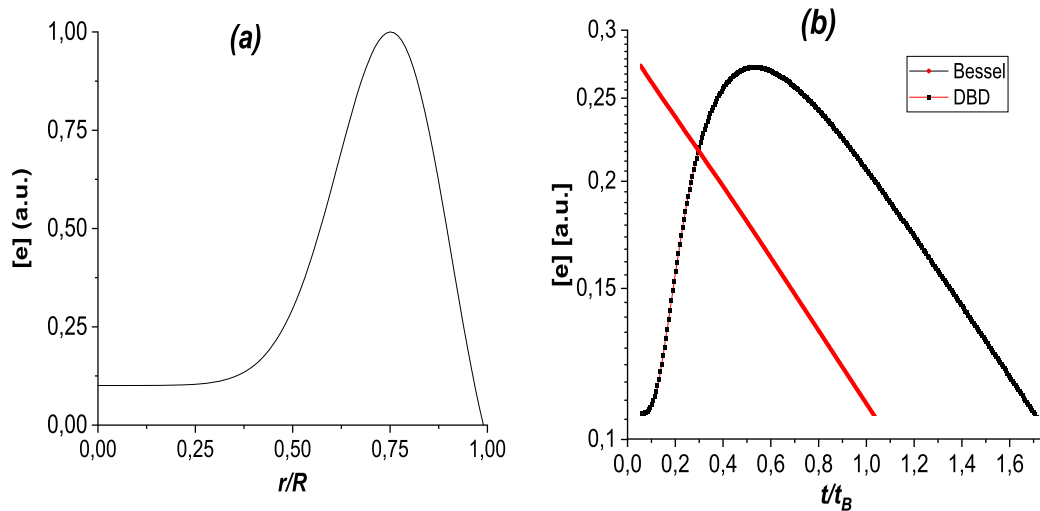
**Figure 2.** (a) The initial distribution of electron density (in arb. units) over the radius. (b) Solutions for the Bessel and created by the DBD electron density distributions on the tube axis. $t_B$ is the diffusion time for $J_0(r/R)$.

noted above, is due to the ambipolar diffusion of charged particles to the boundary of the plasma. In a barrier discharge, the electric field strength and, correspondingly, the ionization rate and plasma electron density are maximal near the electrodes [33, 34]. Therefore, the diffusion motion of charged particles is fundamentally different from diffusion in a plasma produced by DC or microwave discharges in cited above experiments. In the initial phase of the afterglow of such a DBD, the flow of charged particles is directed toward the center of the tube, which, obviously, increases the duration of the afterglow of the plasma in the axial regions, during which its radiation contains information about the recombination processes. Note that it is important to increase the afterglow time, and not the electron density on the axis. The latter is easily achieved simply by increasing the voltage at the electrodes, but this increases the collisional-radiative recombination flux (9) and does not contribute to the solution of the problem. Figure 2(b) shows a numerical solution of the diffusion equation for particles in a cylindrical tube with initial and boundary conditions for the afterglow of DBD (figure 2(a)) approximately describing the experiment. A comparison of the solutions for [e](r) corresponding to the Bessel function $J_0(r/R)$ and created by the DBD, provided that their maximum values on the axis are the same, shows the effectiveness of the DBD in afterglow spectroscopy. In reality, the effect may be slightly smaller, because in the near-wall plasma layers recombination losses may play some role, however, we can assume that they are small, because in the case of low pressures under consideration, the ions are mainly atomic, and the collisional-radiative recombination rate (9) is low. The role of this process will be discussed below.

As shown in figure 1, a coil of inductive discharge operating at a frequency of about 30 MHz was wound over the DBD electrodes. The generator (RF in figure 1) turned on in a pulsed mode with a definite time delay with respect to DBD and 'heated' the electrons in the afterglow. The heating level was set by the power of the pulse. As is known [35, 36], the

electric field of an induction discharge contains two components, $E$ and $H$, which can participate in the acceleration of plasma electrons. Obviously, in the experiment under discussion, in the presence of conducting electrodes along the entire region occupied by the plasma, the heating of electrons is due only to the eddy ($H$) field. We also used a pulsed and stationary RF discharge to create a plasma with the aim of comparing the spectra and afterglow of the RF discharge and the DBD.

The heating of the decaying plasma electrons by a high-frequency field as a tool for studying elementary processes has a long history. It was first demonstrated by the authors of [37, 38] and with its help, data on the recombination rate of helium plasma [39] were obtained in a wide range of electron temperature. An alternative method of pulsed heating of afterglow electrons by a longitudinal electric field of a non-self-sustained discharge was used by us [25, 40, 41] to analyze various elementary processes. It should be noted, however, that at low pressures its use is very problematic. The fact is that the potential fall in the positive column of this discharge can be much smaller than the cathode fall, which, moreover, is not constant in the afterglow. To overcome this problem, we combined the DBD with a pulsed RF discharge. Such a combination has an undeniable advantage both in terms of the simplicity of creating a plasma and the convenience of controlling the level of electron heating in the afterglow by changing the power of the RF generator.

## 3. Results and discussion

### 3.1. The afterglow of RF discharge and the DBD

Figure 3 shows the afterglow of pulsed RF and barrier discharges. The neon pressure is 0.55 Torr, the electron density at the beginning of the afterglow is [e] $\approx 3 \times 10^{10}$ cm$^{-3}$, and the duration of the RF discharge pulse is 10 $\mu$s. The measurements were carried out by the method of multichannel photon counting. The conditions are chosen so that the maximum intensities
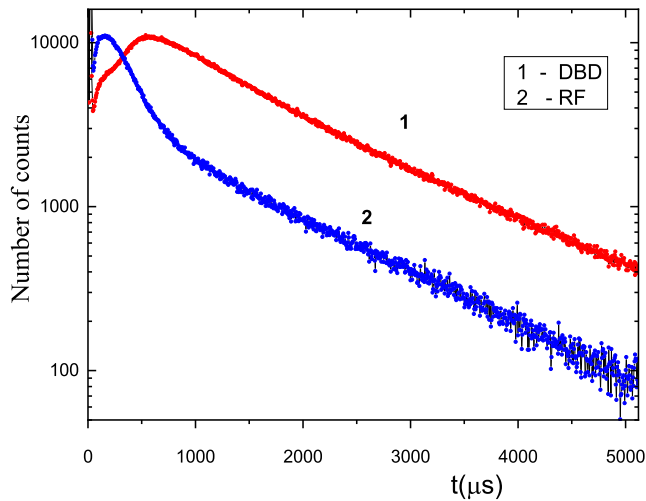
**Figure 3.** Afterglow of RF discharge and the DBD. $P_{Ne} = 0.55$ Torr. $t = 0$ corresponds to the beginning of discharges.



**Figure 4.** Densities of metastable and resonance atoms in the afterglow with pulsed electron heating and model curves for electron concentrations $(2-8) \times 10^{10}$ cm$^{-3}$ $t = 0$ corresponds to the beginning of the DBD.

of the 585.2 nm line (transition $2p_1 \rightarrow 1s_2$ in Paschen notation) in the afterglow of both discharges are the same. One can see a significant difference in the evolution of the afterglow of these discharges. At a qualitative level, this difference clearly correlates with the numerical solution of the diffusion equation (figure 2(b)). These data, in our opinion, show the feasibility of using DBD as a way to create a low-pressure plasma for studying elementary processes at the stage of its decay.

### 3.2. Estimation of the electron density in the afterglow

At this stage of the work, we did not set the task of measuring the temperature and density of the DBD electrons. It seemed important to us to show the advantages of the proposed approach for studying the processes of electron-ion recombination. Therefore, we only give an estimate of the electron density that we obtained in the framework of the OES, supplementing it with resonance absorption spectroscopy. The essence of the method is to observe the response of the populations of $^3P_1$ and $^3P_2$ levels ($s_4$ and $s_5$ in Paschen notation) of the $2p^53s$ configuration to the heating of electrons in the afterglow and to use the known rate constant $k_{21}(T_e)$ of electron-induced $^3P_2 \rightarrow {}^3P_1$ transitions to estimate the electron density [40]

$$k_{21}(T_e) = c_{21} \exp(-\Delta_{21}/T_e)(0.03/T_e)^{0.3}, \qquad (10)$$

$C_{21} = (2.77 \pm 0.15) \times 10^{-7}$ cm$^3$ s$^{-1}$, $\Delta_{21} = 0.052$ eV— energy gap between $^3P_2$ and $^3P_1$ levels. We do not describe this procedure in detail, since it repeats what was done in [40], and the only difference is that in this work, an RF discharge is used to heat electrons. The evolution of densities $[^3P_1]$ and $[^3P_2]$ in the afterglow at the maximal in this work DBD power is shown in figure 4. The data were obtained from optical absorption measurements using the 621.7 nm, 640.2 nm (transitions $2p_7 \rightarrow 1s_5$ and $2p_9 \rightarrow 1s_5$) and 607.4 nm ($2p_3 \rightarrow 1s_4$) lines. A discharge tube with a diameter of 1.5 cm filled with neon at a pressure of 2 Torr and located across the optical axis was used as a supplementary source. Details of the calculation of
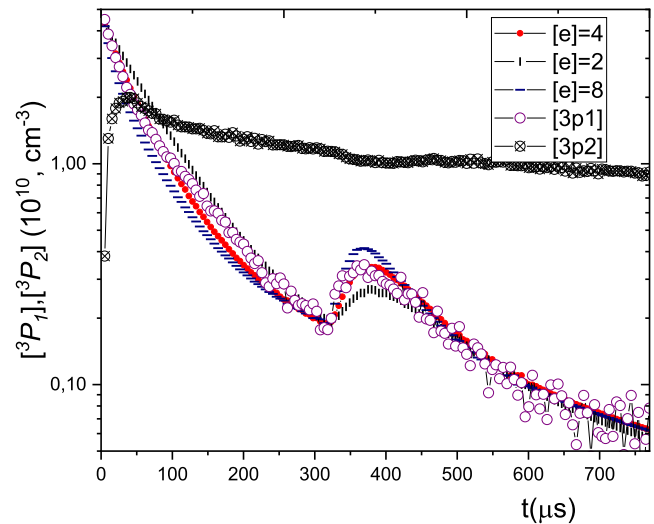
atomic densities in a similar experiment are described in [25]. The level of electron heating in the pulse was chosen so that the rise of the population $[^3P_1](t)$ was close to saturation. As follows from the dependence $k_{21}(T_e)(10)$, this takes place at $T_e \approx 0.1$ eV. At $T_e \geqslant 0.1$ eV, the constant $k_{21}$ depends only slightly on temperature, so that the uncertainty of $T_e$ did not introduce a large error into the estimation of the electron density. We obtained information on the value of [e] by comparing the experimental curves of $[^3P_1](t)$ with model calculations describing the kinetics of $[^3P_1]$ based on a system of differential equations with known rate constants of collisional processes [40]. Diffusion of $^3P_1$ atoms is too slow a process to affect the course of $[^3P_1](t)$ within the time interval of figure 4. The only significant uncertainty in the model parameters is the decay of $^3P_1$ due to the emission of a resonant quantum. As is known [42], the problem of the propagation of resonant radiation is a multi-parameter problem requiring accurate knowledge of the spatial distribution of the population $[^3P_1](r)$. At present, we do not have a solution to such a problem. Therefore, the effective lifetime of escape of 'imprisoned' resonance radiation $\tau_{res}$ was treated together with the electron density as adjustable parameter in the model to be determined through comparison with the experimental observations. The degree of conformity of the model and experiment can be estimated from the data presented in figure 4. The best fit is achieved at [e] $\approx$ $4 \times 10^{10}$ cm$^{-3}$. As $\tau_{res}$, a value of 250 $\mu$s was found and used in all model calculations. Given the spatial distribution uncertainty $[^3P_1](r)$, it is difficult to assess the extent to which this result matches the predictions of Holstein's [42] theory. We only note that, in order of magnitude, the value of $\tau_{res}$ is in reasonable agreement with the experimental results presented in [43].

For our experiments, the model gives [e] $\leqslant 4 \times 10^{10}$ cm$^{-3}$ in the center of the discharge tube. We estimate the accuracy of determining the electron density using this procedure
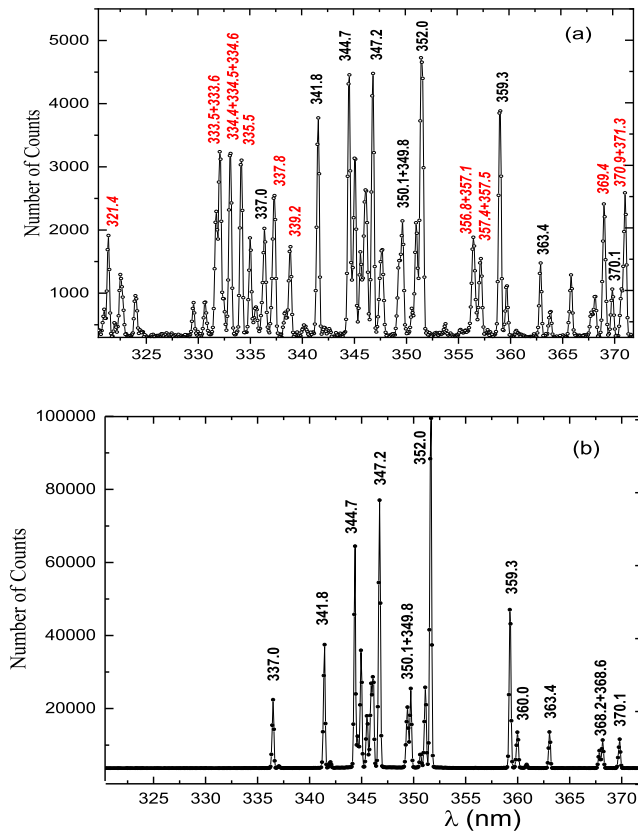
**Figure 5.** The DBD time-integrated spectrum at a frequency of 80 Hz (a) and RF (b) discharges. The strongest $(Ne^+)^*$ lines are marked in red. $P_{Ne} = 0.55$ Torr.

at 30%. Note that the level of electron heating in the experiments under discussion did not go beyond the limits of the typical for recombination afterglow decreasing dependence of the spectral line brightness on $T_e$ (see below).

### 3.3. Spectra of RF discharge and the DBD

The difference in the mechanisms of DBD plasma formation from RF and DC low-pressure discharges is reflected in the spectral characteristics of radiation of both the active stage and the afterglow. In all previous studies of the afterglow of weakly ionized plasma, the authors observed the emission of exclusively neutral excited atoms. In our version of the DBD, it was possible to observe the emission of excited ions $(Ne^+)^*$ associated with the recombination of doubly charged ions

$$Ne^{++} + e + e \rightarrow (Ne^+)^* + e \qquad (11)$$
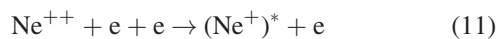
This feature of the DBD is especially pronounced in the short-wavelength region of the spectrum. Figure 5 shows a very noticeable enrichment of the plasma emission spectrum in the case of DDB. The discharges parameters were the same as when registering their afterglow (figure 3). The afterglow of the ion emissions, as will be seen, differs markedly from that of the neon atom. The brightest ion lines and the upper levels of the $(Ne^+)^*$ ion are listed in correspondence with NIST database in table 1.

**Table 1.** The brightest ion lines in the DBD spectrum at a neon pressure of 0.55 Torr.

| Line, nm | Upper level Config.,Term, $J$ | | | Upper level Energy, eV |
|---|---|---|---|---|
| 321.4 | $2s^2 2p^4(^3P)3d$ | $^4F$ | 5/2 | 34.814 4203 |
| 333.5 | $2s^2 2p^4(^3P)3p$ | $^4D^\circ$ | 7/2 | 30.885 5315 |
| 334.5 | $2s^2 2p^4(^1D)3p$ | $^2P^\circ$ | 3/2 | 34.253 9618 |
| 335.5 | $2s^2 2p^4(^3P)3p$ | $^4D^\circ$ | 5/2 | 30.927 3575 |
| 337.8 | $2s^2 2p^4(^3P)3p$ | $^2P^\circ$ | 1/2 | 31.528 2104 |
| 339.2 | $2s^2 2p^4(^3P)3p$ | $^2P^\circ$ | 3/2 | 31.512 4421 |
| 356.8 | $2s^2 2p^4(^1D)3p$ | $^2F^\circ$ | 7/2 | 34.022 3899 |
| 357.5 | $2s^2 2p^4(^1D)3p$ | $^2F^\circ$ | 5/2 | 34.016 8697 |
| 369.4 | $2s^2 2p^4(^3P)3p$ | $^4P^\circ$ | 5/2 | 30.523 9687 |
| 370.9 | $2s^2 2p^4(^3P)3p$ | $^4P^\circ$ | 1/2 | 30.574 2155 |
| 371.3 | $2s^2 2p^4(^3P)3p$ | $^2D^\circ$ | 5/2 | 31.121 4161 |

### 3.4. Active stage and early afterglow of the DBD

Figure 6 illustrates the temporal evolution of spectral intensities $J_i(t)$ of the axial part of the tube during the discharge and early afterglow. The presence of two intensity maxima reflects the sequence of ionization and excitation of atoms by two voltage half-waves of different polarity on DBD electrodes. The large difference in the rates of change of intensities in the active stage and after its completion indicates a difference in the mechanisms of excitation of atomic levels. At neon pressure $P_{Ne} < 1$ Torr, the relaxation time of the electron temperature due to elastic collisions with atoms is several hundred microseconds, so the data in figure 6 relate to the initial stage of relaxation of $T_e(t)$. The change in the decay rate with time is obviously due to the difference in the dependences of the excitation rates and the spectral intensities on the electron temperature $J_i(T_e) \sim \exp(-\varepsilon_j/kT_e)$. In the case of a direct process, the excitation energies of the 4d and 3p levels of the neon atom differ by $\approx 10\%$ and amount to $\varepsilon_i \approx 20$ eV. For stepwise excitation from metastable and resonant states of the $2p^5 3s$ configuration, the energies $\varepsilon_{4d}$ ($\approx 4$ eV) and $\varepsilon_{3p}$ ($\approx 2$ eV) differ by a factor of two, and this difference is reflected in the decay rates of the intensities of the considered lines after the active stage. Ion emissions, of course, react more strongly to changes in electron temperature.

### 3.5. Late afterglow.

Figure 7 shows the complete picture of the afterglow at some of the transitions studied. The energy levels of excited $Ne^*$ atoms and the studied spectral lines are shown in figure 8. The time behavior $J_i(t)$ of the intensities of atomic lines is fully consistent with the studies cited above in the sense that there is a clear correlation between their dependencies on time and the location of the upper level of the line with respect to the ground vibrational level $v = 0$ of the molecular ion. The DR is associated with the population of only those atomic levels that are located lower than the ground vibrational level of the molecular ion. The authors of [45, 46] explain this by the high relaxation rates of populations of vibrational levels of molecular ions in collisions with atoms and electrons. According to [22, 23], a significant fraction of the $Ne_2^+$ recombination flux goes to the $2p_1$ level, emitting a line of 585.2 nm.
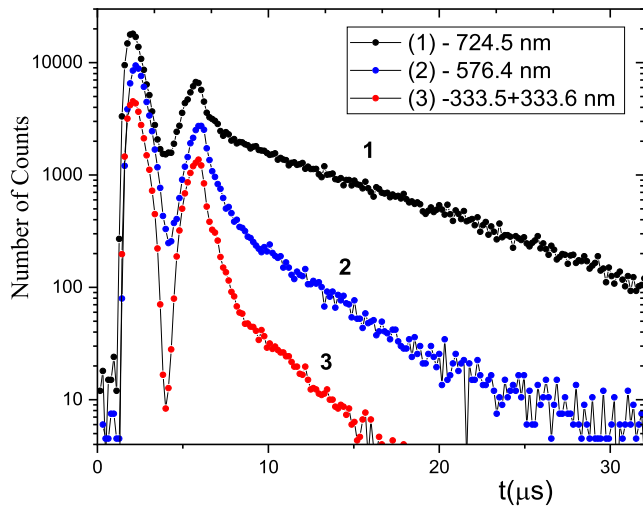
**Figure 6.** Evolution of the DBD plasma emission at 4d → 3p (576.4 nm), 3p → 3s (724.5 nm) transitions of the neon atom and the intensity of the unresolved in this experiment lines 333.5 + 333.6 nm of the $(Ne^+)^*$. The channel width is 0.16 $\mu$s. $P_{Ne} = 0.65$ Torr. $t = 1.28$ $\mu$s corresponds to the beginning of the DBD.



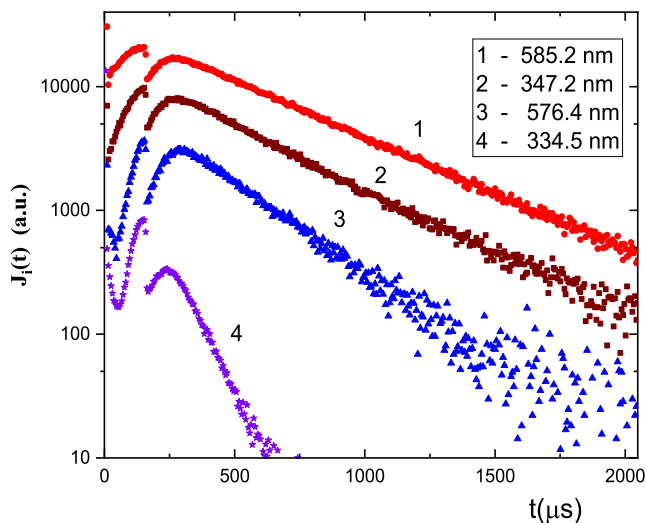**Figure 7.** Spectral intensities in the afterglow. Pressure $P_{Ne} = 0.65$ Torr. [e] ($t = 0$) ≈ $4 \times 10^{10}$ cm$^3$. 4—the intensity of unresolved in this experiment lines 334.4, 334.5, and 334.6 nm of $(Ne^+)^*$. $t = 0$ correspond to the beginning of the DBD.

The same time behavior, as seen from figure 7 also show emissions from the lower 4p levels, including 347.2 nm [25].

The 4d levels are situated more than 0.4 eV above $Ne_2^+$ ($v = 0$) and, at electron temperatures $T_e \approx 300$ K, are inaccessible for the DR of $Ne_2^+$ ions. Their population in the afterglow is due to the collisional-radiative recombination (9). According to [47] and later calculations [48], for an electron density [e] $\geqslant 3 \times 10^{10}$ cm$^{-3}$, the dependence $\alpha_{cr}(T_e)$ is close to $\sim T_e^{-4.5}$, and its value at $T_e = 300$ K $\alpha_{cr} \approx 10^{-9}$ cm$^3$ s$^{-1}$. This applies equally to process (11). Therefore, we can expect that not only the time course, but also the response of the line intensities associated with processes (9) and (11) to a change in the electron temperature in the afterglow will differ from the
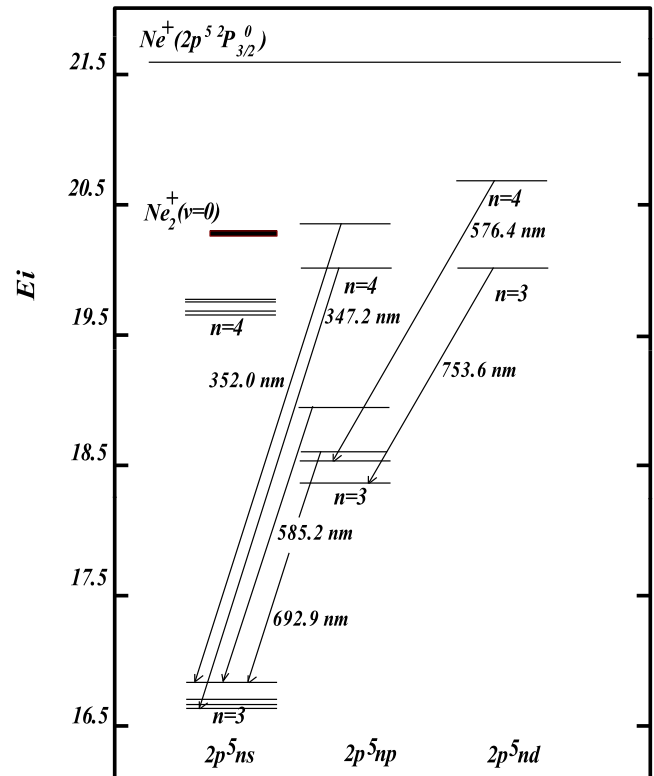


**Figure 8.** A diagram of the neon atom excited levels and the energies of atomic and molecular ions. The position of the vibrational level $v = 0$ of the molecular ion is indicated in accordance with the results of [44].

behavior of the emissions of 3p and 4p levels. This is shown by the data in figure 7 from which, in particular, it is seen that the response to the heating of electrons of the populations [$Ne_{4d}^*$] and [$(Ne^+)^*$], i.e. products of collisional-radiative recombination of $Ne^+$ and $Ne^{++}$ ions are the same. All the other $(Ne^+)^*$ emissions exhibited the same time behavior as shown in figure 7.

Figure 9 shows the 692.9 nm spectral line intensity (transition $2p_6 \to 1s_2$ in Paschen notation) in the afterglow with electron heating by pulses of various duration and power. With an increase of the RF power, the transition from the recombination branch of the temperature dependence of intensities to stepwise excitation by electron impact is easily carried out. It can be seen that after prolonged electron heating, the brightness of the afterglow decreases by more than an order of magnitude. This is due to an increase of the ambipolar diffusion rate with increasing $T_e$ (as is known, the coefficient of ambipolar diffusion $D_a$ is proportional to $T_e$).

The difference in the temporal behavior of the intensities $J_{3p,4p}(t)$ and $J_{4d}(t)$, which is clearly observed in the experiment, is understandable on a qualitative level and data on elementary processes available in the literature are quite sufficient to explain it. The kinetics of the $Ne^{++}$ ions is another matter. In accordance with the theory of collisional-radiative recombination, the rates of processes (9) and (11) are of the same order of magnitude, i.e., the decay of the $Ne^{++}$ ions is not associated with recombination losses. This means that the observed much faster decay of the density [$Ne^{++}$] in comparison with
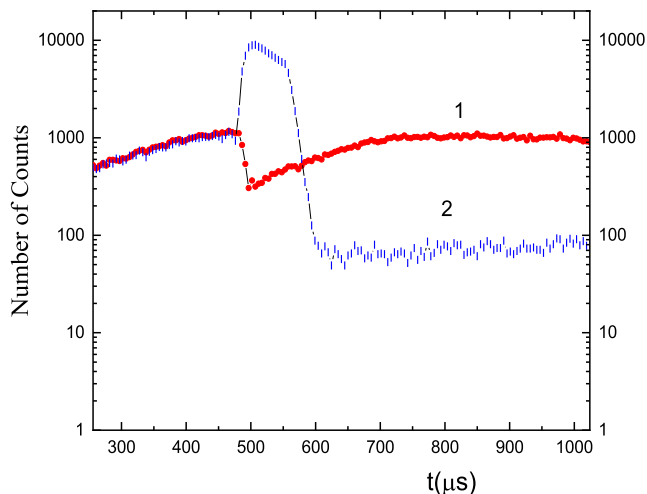
**Figure 9.** 692.9 nm spectral line intensity in the afterglow. Pressure $P_{Ne} = 0.65$ Torr. The pulse duration of the RF is 10 $\mu$s (1) and 80 $\mu$s (2), the RF coil (figure 1) voltage is 30 V (1) and 85 V (2). $t = 0$ corresponds to the beginning of the DBD.

other ions in the afterglow is due to their interaction with surrounding particles. We do not have such data at present. More detailed information on the kinetics of $Ne^{++}$ ions in plasma we hope to obtain in our following experiments. As regards the main objective of the work, we believe that the presented experimental material clearly demonstrates the advisability of using the DBD-RF discharge combination to study processes in a decaying low-pressure plasma. In the DBD, as is known, the electrical energy coupled into a plasma is mainly transferred to electrons, while the neutral gas remains at ambient temperatures. In our experiments, another important property of the DBD was revealed: at low gas pressure, the energy of the electrons of the barrier discharge is sufficient to create doubly ionized atoms in the plasma.

## 4. Conclusions

We present the results of an experiment on testing a new instrument for studying processes in a decaying plasma—a low-frequency DBD of a cylindrical configuration combined with a pulsed inductive RF discharge. Neon pressure is less than 1 Torr, electron density [e] $\leqslant 0.4 \times 10^{10}$ cm$^{-3}$. The methods of optical emission spectroscopy were used to study the afterglow of the DBD with pulsed heating of electrons by an RF field. The difference in the temporal behavior of the spectral line intensities together with their reaction to temperature disturbances was used to identify the recombination mechanisms of population of neon excited levels in the plasma with atomic and molecular ions. The advantages of the proposed experimental setup for solving the problem of the role of the dissociative recombination of molecular ions in the formation of the optical characteristics of the plasma are discussed. It has been shown for the first time that the low pressure neon plasma produced by DBD contains $Ne^{++}$ ions, the recombination of which with electrons noticeably enriches the afterglow spectrum.

## References

[1] Biondi M A and Brown S C 1949 Measurements of ambipolar diffusion in helium *Phys. Rev.* **75** 1700
[2] Kokoouline V, Ayouz M, Mezei J Z, Hassouni K and Schneider I F 2016 Theoretical study of dissociative recombination and vibrational excitation of the BF$^+_2$ ion by an electron impact *Plasma Sources Sci. Technol.* **27** 115007
[3] Lebedev V S, Kislov K S and Narits A A 2018 Strong enhancement of electron–ion recombination owing to free–bound and bound–bound resonance transitions *JETP Lett.* **108** 582
[4] Shon J W, Rhoades R L, Verdeyen J T and Kushner M J 1993 Short pulse electron beam excitation of the high-pressure atomic Ne laser *J. Appl. Phys.* **73** 8059
[5] Frommhold L, Biondi M A and Mehr F J 1968 Electron-temperature dependence of electron-ion recombination in neon *Phys. Rev.* **165** 44
[6] Shiu Y J and Biondi M A 1978 Dissociative recombination in argon *Phys. Rev.* A **17** 868
[7] Shiu Y J and Biondi M A 1977 Dissociative recombination in kripton *Phys. Rev.* A **16** 1817
[8] Syiu Y J, Biondi M A and Sipler D P 1977 Dissociative recombination in xenon *Phys. Rev.* **15** 494
[9] Dahler J S, Franklin J L, Munson M S B and Field F H 1962 Rare-gas molecule-ion formation by mass spectrometry. Kinetics of Ar$^{2+}$, Ne$^{2+}$, and He$^{2+}$ formation by second-and third-order processes *J. Chem. Phys.* **36** 3332
[10] Sauter G F, Gerber R A and Oskam H J 1966 Studies of decaying plasmas produced in Ne and He-Ne mixtures *Physica* **32** 1921
[11] Veatch G E and Oskam H J 1970 Recombination and ion-conversion processes in helium-neon mixtures *Phys. Rev.* A **2** 1422
[12] Veatch G E and Oskam H J 1970 Recombination and ion-conversion processes of argon ions *Phys. Rev.* A **1** 1498
[13] Hornbeck J A and Molner J P 1951 Mass spectrometric studies of molecular ions in the noble gases *Phys. Rev.* **84** 621
[14] Huffman R E and Katayama D H 1966 Photoionization study of diatomic-ion formation in argon, krypton, and xenon *J. Chem. Phys.* **45** 138
[15] Biondi M A 1951 Ionization by the collision of pairs of metastable atoms *Phys. Rev.* **82** 453
[16] Akoshile C O, Clark J D and Cunningham A J 1986 Reactions of excited atoms of neon in neon-helium afterglows: II. Kinetic model *J. Phys. B: At. Mol. Phys.* **19** 349
[17] Neynaber R H, Magnuson G D and Tang S Y 1978 Chemi-ionization in collisions of metastable helium with metastable helium *J. Chem. Phys.* **68** 5112
[18] Deloche R, Monchicourt P, Cheret M and Lambert F 1976 High-pressure helium afterglow at room temperature *Phys. Rev.* A **13** 1140
[19] Connor T R and Biondi M A 1965 Dissociative recombination in neon: spectral line-shape studies *Phys. Rev.* **140** 778
[20] Frommhold L and Biondi M A 1969 Interferometric study of dissociative recombination radiation in neon and argon afterglows *Phys. Rev.* **185** 244

[21] Ciurylo R, Bielski A, Domyslawska J, Szudy J and Trawinski R S 1994 Effect of dissociative recombination on spectral line profiles in neon glow discharge *J. Phys. B: At. Mol. Opt. Phys.* **27** 4181

[22] Steenhuijsen L W G, Van Schaik N, Van de Nieuwenhuyzen L C A M and Verspaget F H P 1979 Measurments of the production of neon 2p atoms by dissociative recombination *J. Phys. Colloq.* **40** C7–95

[23] Malinovský L, Lukáč P and Hong C J 1986 Production of the excited Ne(2p 53p) atoms by dissociative recombination in the afterglow of high frequency neon discharge *Czech. J. Phys.* **36** 1035

[24] Malinovsky L, Lukac P, Trnovec J, Hong C J and Talsky A 1986 Population of the excited Ne atoms in 3d levels by dissociative recombination in the neon afterglow plasmas at room temperature *Czech. J. Phys.* **40** 1036

[25] Gordeev S V, Ivanov V A and Skoblo Yu E 2019 Dissociative recombination of molecular Ions with electrons: population of Ne(2p$^5$4p) atoms in a decaying plasma *Optic Spectrosc.* **127** 418

[26] Ramos G B, Schlamkowitz M, Sheldon J, Hardy K A and Peterson J R 1995 Observation of dissociative recombination of Ne$_2^+$ and Ar$_2^+$ directly to the ground state of the product atoms *Phys. Rev.* A **51** 2945

[27] Ramos G, Sheldon J W, Hardy K A and Peterson J R 1997 Dissociative-recombination product states and the dissociation energy D$_0$ of Ne$_2^+$ *Phys. Rev.* A **56** 1913

[28] Ivanov V A 1992 Dissociative recombination of molecular ions in noble-gas plasmas *Sov. Phys. Usp.* **35** 18

[29] Florescu-Mitchell A I and Mitchell J B A 2006 Dissociative recombination *Phys. Rep.* **430** 277

[30] Ivanov V A 2019 Barrier discharge in helium at medium pressures. Afterglow spectroscopy *Optic Spectrosc.* **126** 167

[31] Brandenburg R 2017 Dielectric barrier discharges: progress on plasma sources and on the understanding of regimes and single filaments *Plasma Sources Sci. Technol.* **26** 053001

[32] Bazinette R, Subileau R, Paillol J and Massines F 2014 Identification of the different diffuse dielectric barrier discharges obtained between 50 kHz to 9 MHz in Ar/NH3 at atmospheric pressure *Plasma Sources Sci. Technol.* **23** 035008

[33] Golubovskii Yu B, Maiorov V A, Behnke J and Behnke J F 2003 Modelling of the homogeneous barrier discharge in helium at atmospheric pressure *J. Phys. D: Appl. Phys.* **36** 39

[34] Ivković S S B M, Obradović B M and Kuraica M M 2012 Electric field measurement in a DBD in helium and helium–hydrogen mixture *J. Phys. D: Appl. Phys.* **45** 275204

[35] Babat G I 1947 *Electrodeless Discharge and Some Allied Problems* vol 94 (London: IEEE) 27

[36] Park I L-S, Kim K-H, Kim T-W, Kim K-Y, Ho-Jun M and Chin-Wook C 2018 Evolution of two-dimensional plasma parameters in the plane of the wafer during the E- to H- and H- to E-mode transition in an inductively coupled plasma *Plasma Sources Sci. Technol.* **27** 055018

[37] Goldstein L, Anderson J M and Clark G L 1953 Interaction of microwaves propagated through a gaseous discharge plasma *Phys. Rev.* **90** 151

[38] Goldstein L, Anderson J M and Clark G L 1953 Quenching of afterglow in gaseous discharge plasmas by low power microwaves *Phys. Rev.* **90** 486

[39] Chen C L, Leiby C C and Goldstein L 1961 Electron temperature dependence of the recombination coefficient in pure helium *Phys. Rev.* **121** 1391

[40] Ivanov V A 1998 Electron-impact-induced excitation transfer between 3s levels of the neon atom *J. Phys. B: At. Mol. Opt. Phys.* **31** 1765

[41] Ivanov V A and Prikhodjko A S 1991 Dissociation of Xe$_2^+$ molecular ions by electrons in plasma *J. Phys. B: At. Mol. Opt. Phys.* **24** L459

[42] Holstein T 1951 Imprisonment of resonance radiation in gases *Phys. Rev.* **83** 1159

[43] Phelps A V 1959 Diffusion, de-excitation, and three-body collision coefficients for excited neon atoms *Phys. Rev.* **114** 1011

[44] Ivanov V A, Petrovskaya A S and Skoblo Yu E 2019 Dissociation energy and dissociative recombination of Ne$^+_2$ and HeNe$^+$ Ions *J. Exp. Theor. Phys.* **128** 767

[45] Bates D R 1979 Formation of excited helium atoms from helium molecular ions *J. Phys. B: At. Mol. Phys.* **12** L35

[46] Stevefelt J 1973 Three-body capture – autoionization: a mechanism for vibrational deexcitation of molecular ions in a plasma *Phys. Rev.* A **8** 2507

[47] Bates D R and Kingston A E 1961 Recombination through electron-electron collisions *Nature* **189** 652

[48] Stevefelt J, Boulmer J and Delpech J-F 1975 Collisional-radiative recombination in cold plasmas *Phys. Rev.* A **12** 1246